Polarimetric Adaptive Processing and Eigenvalue Detector for Counter UAVs radar

Milan Rozel
DEMR, ONERA, Université de Paris-Saclay – Palaiseau
FRANCE
Milan.Rozel@onera.fr

Philippe Brouard
DEMR, ONERA, Université de Paris-Saclay – Palaiseau
FRANCE
Philippe.Brouard@onera.fr

Hélène Oriot
DEMR, ONERA, Université de Paris-Saclay - Palaiseau
FRANCE
Helene.Oriot@onera.fr

ABSTRACT

The last decade has seen great developments in the domain of small unmanned aerial vehicles (UAVs). Today UAVs are able to carry out a wide range of missions and recent developments in conflict zones, involving states and non-state actors, have shown how effective they can be. This effectiveness lies in part on their ability to foil conventional surveillance systems, as low observable targets. From an air surveillance radar system perspective, low observability of small UAVs results from a very unique combination of a small radar cross section, an ability to fly at low speeds and at low altitudes and to mimic, intentionally or not, natural objects such as birds. Therefore, small UAVs are likely to be endo-clutter targets (targets sharing a similar speed with the clutter), as such challenging to be detected. Detection in low grazing angle scenarios and related radar clutter properties have long been studied. Most of these studies suggest the implementation of adaptive processes in radar detection step in order to cope with dynamic clutter . In this paper, we present experimental results of an ongoing work on counter-UAVs radars addressing the design of an adaptive processing and eigenvalue detector using polarimetric features. Inspired by a method used in SAR imaging target detection, this processing improves detection of endo-clutter clutter targets without prior knowledge or assumption of radar clutter signature.

Keywords— Radar, Polarimetry, Radar Clutter, Eigenvalue Detector, UAV Detection, Signal to Clutter Ratio

1.0 INTRODUCTION

Due to their ease of access and use, small unmanned aerial vehicles (UAVs) pose an important challenge for security. A challenge further accentuated by the potential weakness of radar for their detection. Indeed, as UAVs can fly at low altitude larger ground clutter can be then intercepted by the transmit and receive antennas beam patterns. With higher clutter environment, this low grazing angle geometry, combined with low relative speeds to the radar, can make them endo-clutter targets (target located in the clutter, in our case, relative speed 0 m/s). To make matters even more complicated, other targets such as birds or any mobile objet in the scene can have a similar radar signature and therefore can confuse the radar. Endo-clutter detections are usually addressed in the context of radar imagery with airborne radars or in the context of maritime surveillance, with sea clutter [1]. Operational radar systems usually filter the clutter [2] from its Doppler signature [3]. However, as UAVs sometimes have similar Doppler signature to ground mobile clutter, endo-clutter detection needs to take into account other characteristics such as polarimetric information. For instance, polarimetry is used in weather radar and polarimetric amplitude ratios are used in that case for classification and detection purposes. Synthetic Aperture Radar (SAR) [4-5] uses also polarimetry for instance for surface patch classification and target identification. Finally, polarimetry can improve detection in a maritime context[9]. So far, polarimetric radar are seldom used in a counter-UAV context. In this paper, we discuss several methods to improve the detection rates of endo-clutter targets using polarimetric data. In the first part, we present a detector which uses eigenvalues and then present classical detectors to evaluate against the proposed detector. In the second part we depict the experimental setup and

the measurement campaign. Eventually, we present the detectors' output on real data, and show an interest of polarimetric detectors and in particular the eigenvalue detector for detecting endo-clutters UAVs in low-grazing angle geometry.

2.0 EIGENVALUE DETECTOR AND POLARIMETRIC ADAPTIVE PROCESSING

The Signal-to-Clutter Ratio (SCR) governs endo-clutter detections; therefore, they are independent on the transmitted power. In order to improve the detection performance, while keeping the lowest false alarm rate, we compare two detectors, one exploiting eigenvalues of the clutter polarimetric covariance matrix and the other filtering the clutter thanks to the polarimetric covariance matrix. This approach relies on previous researches, especially on SAR systems, implementing polarimetry for image classification [6].

In this study, we consider dual-polarization monostatic radar with fixed array antenna, transmitting horizontal and vertical polarization and receiving simultaneously co-polar and cross-polar signals. We use Doppler-range-maps data to test the detectors and since the radar is static, the clutter ~~will~~ spread over a limited range of Doppler cells around the zero Doppler. Each cell of the Doppler-range maps contains polarimetric information, identified as follows: Xy (X being the transmitted polarization and y being the received polarization); the four polarizations are Hh, Hv, Vh and Vv (H standing for Horizontal polarization, V for Vertical polarization). Considering the reciprocity property that applies in monostatic configuration, i.e. the scattering matrix is symmetric ($x_{Hv} = x_{Vh}$), only 3 information are considered. Therefore, for each cell, we have:

$$X(\mathrm{d},\mathrm{v},\mathrm{t}) = [x_{Hh}(\mathrm{d},\mathrm{v},\mathrm{t}), x_{Hv}(\mathrm{d},\mathrm{v},\mathrm{t}), x_{Vv}(\mathrm{d},\mathrm{v},\mathrm{t})]^T \quad (1)$$

Where d is the radar range, v the velocity and t the time at which the Doppler-range map is computed. For each cell of interest (cells for which the velocity is low or zero) we compute the covariance matrix as follows:

$$\hat{R}(d,v) = \frac{1}{n}\sum_{i=0}^{n-1} R(d,v,i*\delta t) \quad (2)$$

With δt being the time delay between two consecutive Doppler-range maps. R is defined as:

$$R(d,v,t) = (XX^T)(d,v,t) \quad (3)$$

The eigenvalue decomposition of the covariance matrix writes:

$$\hat{R} = U^{-1}\begin{pmatrix}\lambda_1 & 0 & 0\\ 0 & \lambda_2 & 0\\ 0 & 0 & \lambda_3\end{pmatrix}U \quad (4)$$

With λ_x being the eigenvalue sorted in decreasing order, $\lambda_1 > \lambda_2 > \lambda_3$ and $U = (U_1, U_2, U_3)$, U_x being the eigenvectors.

We introduce the proposed detector as well as two classical polarimetric detectors and a monopolarimetric detector to assess the performances of our detectors.

The first detector we propose is a threshold detector based on the level of the highest eigenvalue:

$$EVA = \frac{\lambda_1}{trace(\hat{R})} \tag{5}$$

The second detector is inspired by Space Time Adaptive Processing [8], but instead of filtering thanks to a space-time covariance matrix we filter thanks to the polarimetric covariance matrix. We call it PAP for Polarimetric Adaptive Processing: it is a polarimetric adapted version of the generalized likelihood ratio test (GLRT). The output power writes:

$$PAP(d,v,t) = \max_S \left(\frac{S^H \widehat{R(d,v)}^{-1} X(d,v,t)}{\sqrt{S^H \widehat{R(d,v)}^{-1} S}} \right) \tag{6}$$

S being the polarimetric steering vector, defined as follows:

$$S = \left(A, Be^{j\phi_{cx}}, Ce^{j\phi_{cc}}\right) \tag{7}$$

With ϕ_{cx}being the phase between copolar and crosspolar terms, ϕ_{cc} being the phase between both copolar data channels and A, B and C being defined as follows:

$$\begin{cases} A = \sin\theta \cos\phi \\ B = \sin\theta \sin\phi \\ C = \cos\theta \end{cases} \tag{8}$$

With θ and ϕ being sampled between 0 and $\frac{\pi}{2}$.

The two classical polarimetric detectors are:
The span detector, defined as follows:

$$SPAN(d,v,t) = \frac{|x_{Hh}(\mathrm{d,v,t})|^2 + |x_{Hv}(\mathrm{d,v,t})|^2 + |x_{Vv}(\mathrm{d,v,t})|^2}{trace\left(\hat{R}(d,v)\right)} \tag{9}$$

And the maximum likelihood (ML) detector [3]:

$$ML(d,v,t) = \sqrt{X(d,v,t)^H \widehat{R(d,v)}^{-1} X(d,v,t)} \tag{10}$$

Finally we have standard CA-CFAR in polarisation Hh (the most favourable case for monopolarimetric detection here) to compare the polarimetric detectors to a monopolarimetric counter-part.

3.0 EXPERIMENTAL SETUP AND MEASUREMENTS

3.1 Experimental setup

The radar demonstrator system used to record the data is Hycam (Figure 1). It is an S-band radar demonstrator located on the roof of a building at ONERA, in Palaiseau, France. It was designed by ONERA under a contract of the French Ministry of Armed Forces to investigate new radar concepts and collect radar signatures of both clutter and flying targets. Its main characteristics and features are summed up in Table 1.

More details can be found in [7]. During the experiment the radar was as presented in Figure 1, i.e. with transmit and receive antennas vertically oriented. Several configurations have been tested including MIMO (Multiple Input Multiple Output). The detector discussed in this paper was tested in SIMO (Single Input Multiple Output) mode, i.e. using the same waveform over the 6 transmit channels. Hence the transmit antenna beam pattern was 10° wide in azimuth and 4° in elevation.

Table 1 HYCAM main characteristics

Operating band	S
Instantaneous bandwidth	Up to 500 MHz
Peak power	700 W
Duty cycle	Up to 30% - CW mode available
Tx/Rx arrays	Active Tx array : 12 columns electronically steerable + fully polarimetric (Linear/Circular basis) – splittable in 6 independent sub-arrays Rx array : 16 configurable column : Σ,Δ, H, V
Positionner – Max velocity	Azimuth 90°/s – Elevation 10°/s
ADC	12 bits @2 GS/s / analog bandwidth : 2 GHz / 4 channels

Figure 1: *HYCAM radar*

3.2 Measurements

Testing of the detectors was conducted using dwells with 10 MHz bandwidth 10 µs pulses width and a PRI (Pulse Repetition Interval) of 100µs. The environment of the measurements was semi-urban (Figure 2), with a predominance of non-urban clutter. It contains forested areas, fields, roads and buildings.

The UAV used for the measurements flew along predefined trajectories at a distance of roughly 4km from the radar. It flew along circles of 150m of diameter and along hippodromes of length 250m and width 80m

both perpendicular and parallel to the aiming axis of the radar. The drone flew at 5m/s.

Figure 2 Map with HYCAM position and the UAV position during the measurement. The aiming line is the blue line and the orange lines are the limits of the main lobe.

4.0 EXPERIMENTAL RESULTS

The data are recorded over 800 seconds. Doppler-range maps integration time is 400ms, resulting in 2000 polarimetric Doppler-range maps (see example of a Doppler range map in Figure 3). For each set of 10 consecutive Doppler range maps, the covariance matrices are evaluated for each range cell of the clutter. To take into account the fact that the eigenvalue detector performs a multi-look implicitly when the covariance matrix is computed, we compare the output of the detectors with a similar multi-look. Each detector output shown in the following is the output of the detector averaged over 10 consecutive looks (to correspond the covariance matrix estimation time) to ensure a fair comparison between with the eigenvalue detector.

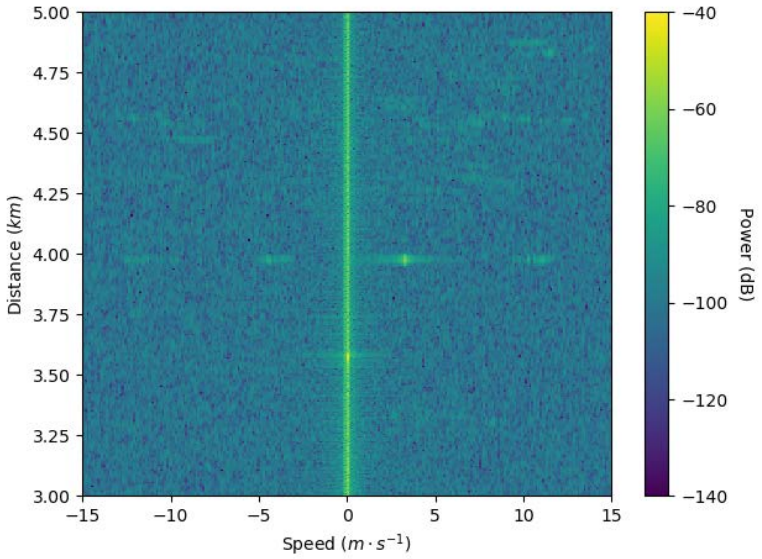

Figure 3 Doppler-range map (Hh polarisation). At the center we can see the clutter and the UAV at 4km and 4m/s as well as its moving parts.

The results are presented at two different range cells. Figure 4, shows over time the detections of the 3

detectors for ranges between 4.05 and 4.25 km, at zero Doppler. In this time span, the UAV crossed the clutter 4 times, at respectively 430 seconds, 475 seconds, 550 seconds and 583 seconds (respectively crossings A, B, C and D). We can see that the eigenvalue detector seems to give better results on the crossing at 4.12 km

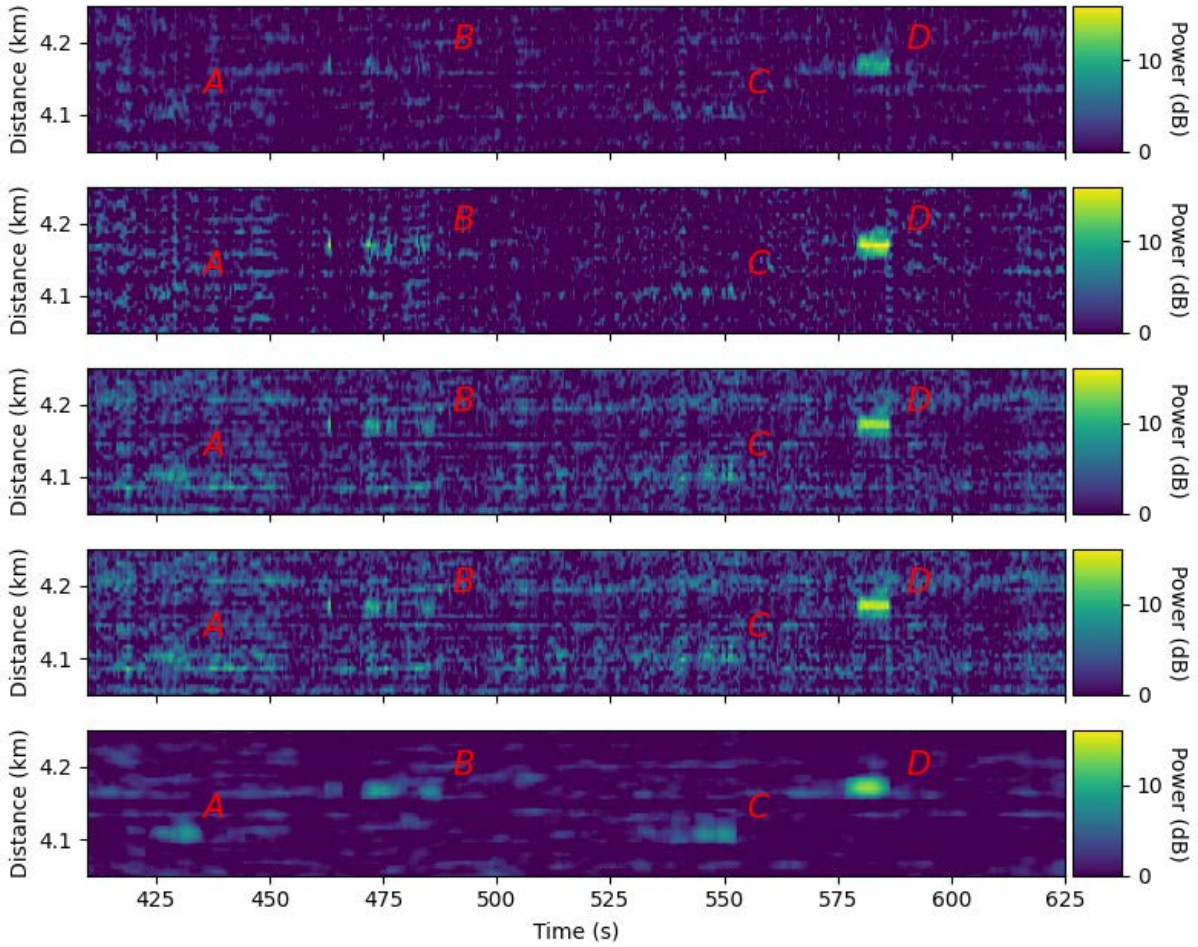

Figure 4 Comparison between span (1st), Monopolar (2nd), Maximum Likelihood (3rd), Polarimetric Adaptive Processing (4th) and Eigenvalue (5th) detector in the clutter.

If we take a closer a look at the range cell at 4.17 km (Crossing D, Figure 5) we can see that the levels of the ML (Maximum Likelihood), PAP (Polarimetric Adaptive Processing) and eigenvalue detector are similar and superior to the level of the span detector.

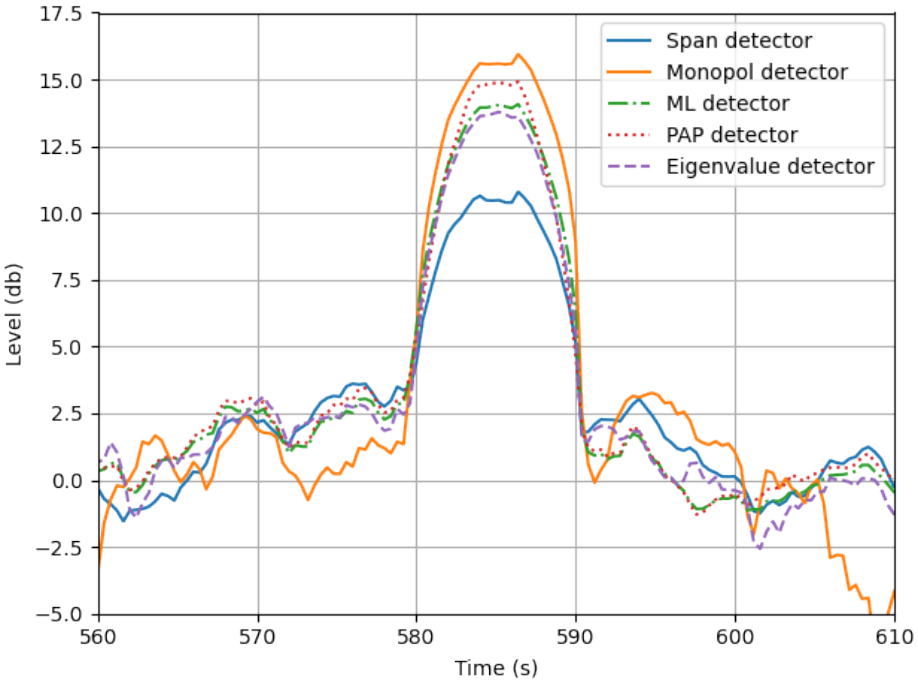

Figure 5 Level comparison between ML, PAP, monopolar, span and eigenvalue detectors at 4.17 km in the clutter (crossing D)

For the range cell at 4.12 km, the level of the 4 detectors are significantly closer. Yet, it appears that the eigenvalue should have lower false alarm rate (Crossings A and C, Fig. 6 and 7).

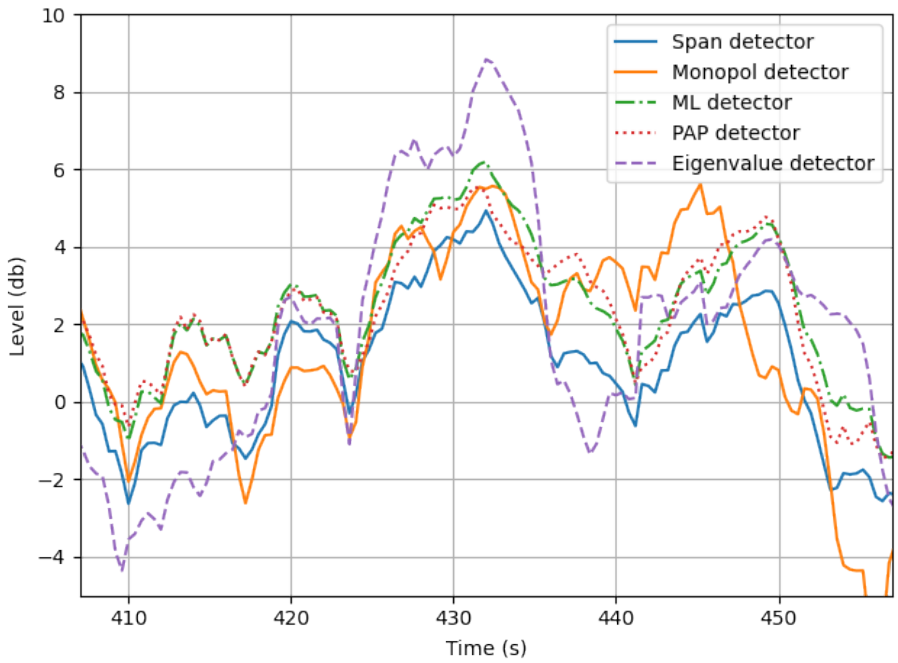

Figure 6 Level comparison between ML, PAP, monopolar, span and eigenvalue detectors for the first crossing at 4.12 km in the clutter (crossing A)

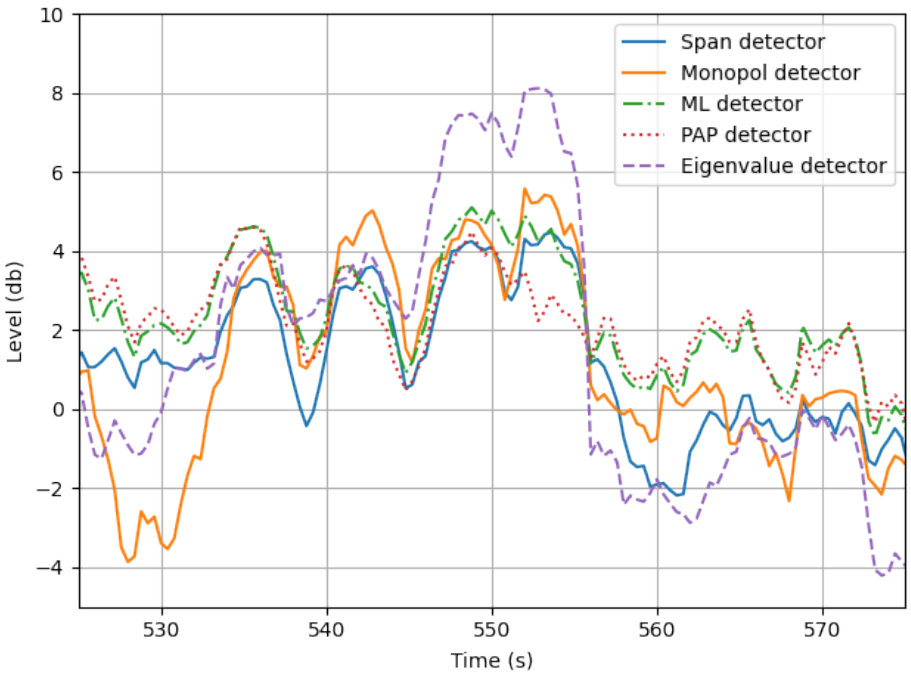

Figure 7 Level comparison between ML, PAP, monopolar, span and eigenvalue detectors for the first crossing at 4.12 km in the clutter (crossing C)

To assess if the False Alarm Rate (FAR) is lower, we estimated the FAR for a given level of each detector. This estimation was made on secondary data assumed not to contain any target (Figure 8).

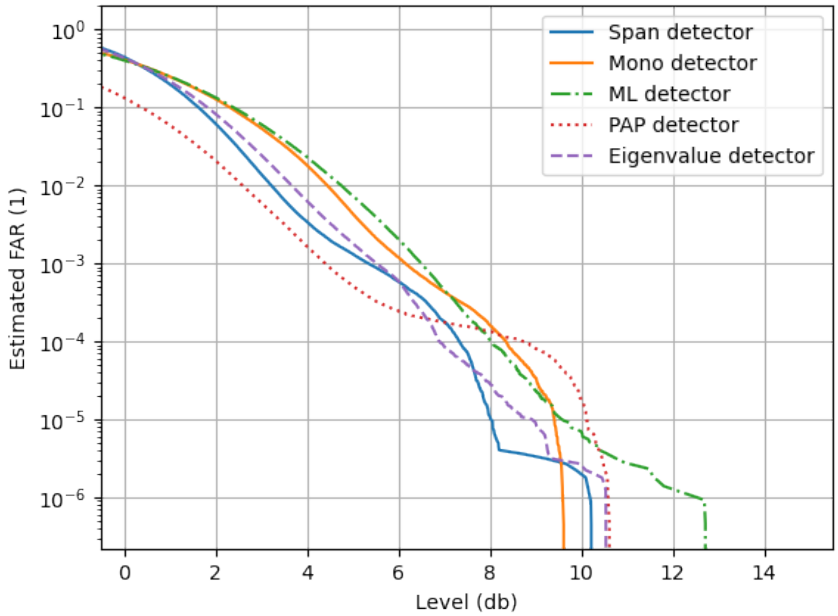

Figure 8 False Alarm Rate estimation for the different detectors.

For a given level, the eigenvalue detectors shows a lower estimated false alarm rate than span and ML detectors, while the PAP show higher false alarm rates (Figure 8). The Table 2 shows that for each crossing location, the estimated False Alarm Rate (FAR) for the eigenvalue detector is better or similar to the ML estimated one and better than the FAR of the span, while the PAP doesn't perform as well as the other detectors. Due to the methodology of this study we have a low sample size for the detections, therefore, we cannot compute Receiver Operating Characteristics (ROC), and cannot compute probability of detection (P_D) adequately. As the FAR estimation is sensitive to selected secondary data set and we cannot ensure a clean secondary data set without censoring a lot of data, the results should be considered carefully, and need further consolidation to be confirmed.

Table 2 Estimated False Alarm Rate for each crossing location

Detector	Estimated false alarm rate			
	A	B	***C***	***D***
Monopolar	$10^{-2.7}$	$10^{-5.3}$	$10^{-2.7}$	$< 10^{-6}$
Span	$10^{-2.8}$	10^{-3}	$10^{-2.7}$	$< 10^{-6}$
Maximum Likelihood	$10^{-2.8}$	$10^{-4.4}$	$10^{-2.2}$	$< 10^{-6}$
Polarimetric Adaptive Processing	$10^{-3.5}$	10^{-4}	10^{-3}	$< 10^{-6}$
Eigenvalue detector	10^{-5}	10^{-5}	$10^{-4.5}$	$< 10^{-6}$

5.0 CONCLUSION

We have been able to test the polarimetric detectors and a mono-polarization detection algorithm with experimental data,. The polarimetric eigenvalue detector discussed in this paper gives better results than both ML and span detectors for endo-clutter targets in low-grazing angle geometries and semi-urban environment. It also gives better or similar performances to the mono-polarization detector meaning that polarization is a tool that can enhance to enhance endo-clutter detections.

By contrast, PAP gives overall inferior performances to the other polarimetric detectors. These detectors will be further investigated, using additional data featuring a larger diversity of the radar system and simulated data.

ACKNOWLEDGEMENT

The authors wish to thank the French Ministry of Armed Forces for funding this PhD thesis.

REFERENCES

[1] H. Leong and A. Ponsford, "The effects of sea clutter on the performance of HF Surface Wave Radar in ship detection," 2008 IEEE Radar Conference, 2008, pp. 1-6, doi: 10.1109/RADAR.2008.4720865.

[2] K. Friedrich, U. Germann, et P. Tabary, « Influence of Ground Clutter Contamination on Polarimetric Radar Parameters », Journal of Atmospheric and Oceanic Technology, vol. 26, no 2, p. 251 269, févr. 2009, doi: 10.1175/2008JTECHA1092.1.

[3] C. Berthillot, A. Santori, O. Rabaste, D. Poullin and M. Lesturgie, "DVB-T Airborne Passive Radar:

clutter block rejection," 2019 International Radar Conference (RADAR), 2019, pp. 1-5, doi: 10.1109/RADAR41533.2019.171365.

[4] L. M. Novak, M. B. Sechtin, et M. J. Cardullo, « Studies of target detection algorithms that use polarimetric radar data », IEEE Transactions on Aerospace and Electronic Systems, vol. 25, no 2, p. 150 165, mars 1989, doi: 10.1109/7.18677.

[5] B. Zakeri, A. Ghorbani, et M. Galletti, « Pure Target Detection Based on Eigenvector Decomposition Using H-α Method in Radar Polarimetry », in 2006 International RF and Microwave Conference, sept. 2006, p. 101 105. doi: 10.1109/RFM.2006.331047.

[6] S. R. Cloude et E. Pottier, « A review of target decomposition theorems in radar polarimetry », IEEE Transactions on Geoscience and Remote Sensing, vol. 34, no 2, p. 498 518, mars 1996, doi: 10.1109/36.485127.

[7] P. Brouard, L. Constancias, A. Brun, S. Attia, J. Peyret, et P. Dreuillet, « Hycam: A new S band surface radar testbed », in IET International Radar Conference 2013, avr. 2013, p. 1 4. doi: 10.1049/cp.2013.0225.

[8] J. Ward, "Space-time adaptive processing for airborne radar," IEE Colloquium on Space-Time Adaptive Processing (Ref. No. 1998/241), 1998, pp. 2/1-2/6, doi: 10.1049/ic:19980240.

[9] V. Meslot, V. Corretja, S. Kemkemian, J.-M. Quellec, R. Montigny, and C. Cochin, “Polarisation influence on sea clutter properties and radar detection performance in X-band for low grazing angles,” in 2016 IEEE Radar Conference (RadarConf), Philadelphia, PA, May 2016, pp. 1–5. doi: 10.1109/RADAR.2016.7485250.